



A Journal of the Gesellschaft Deutscher Chemiker

# Angewandte Chemie

GDCh

International Edition

[www.angewandte.org](http://www.angewandte.org)

## Accepted Article

**Title:** Pnictogens Based Biosensor: Phosphorene, Arsenene, Antimonene, and Bismuthene

**Authors:** Martin Pumera

This manuscript has been accepted after peer review and appears as an Accepted Article online prior to editing, proofing, and formal publication of the final Version of Record (VoR). This work is currently citable by using the Digital Object Identifier (DOI) given below. The VoR will be published online in Early View as soon as possible and may be different to this Accepted Article as a result of editing. Readers should obtain the VoR from the journal website shown below when it is published to ensure accuracy of information. The authors are responsible for the content of this Accepted Article.

**To be cited as:** *Angew. Chem. Int. Ed.* 10.1002/anie.201808846  
*Angew. Chem.* 10.1002/ange.201808846

**Link to VoR:** <http://dx.doi.org/10.1002/anie.201808846>  
<http://dx.doi.org/10.1002/ange.201808846>

## COMMUNICATION

# Pnictogens Based Biosensor: Phosphorene, Arsenene, Antimonene, and Bismuthene

Dedicated to memory of Prof. Emil Paleček, founder of electrochemistry of DNA

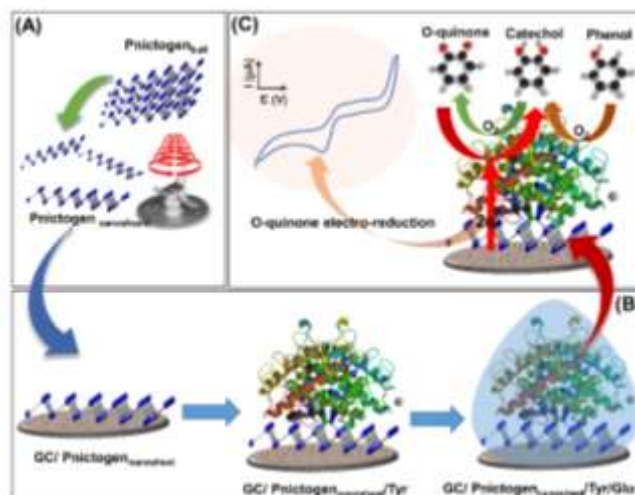
Carmen C. Mayorga-Martinez,<sup>[a]</sup> Rui Gusmão,<sup>[a]</sup> Zdeněk Sofer,<sup>[a]</sup> and Martin Pumera,<sup>\*[a]</sup>

**Abstract:** Two dimensional materials have allowed for great advances in the biosensors field and to obtain sophisticated, smart, and miniaturized devices. In this work, we optimized a highly sensitive and selective phenol biosensor using 2D pnictogens (phosphorene, arsenene, antimonene and bismuthene) as sensing platforms. Exfoliated pnictogen were obtained by the shear force method, undergoing delamination and downsizing to thin nanosheets. Interestingly, compared with the other tested elements, antimonene exhibited the highest degree of exfoliation and the lowest oxidation-to-bulk ratio, to which we attribute its enhanced performance in the phenol biosensor system reported here. The proposed design represents the first biosensor approach developed using exfoliated pnictogens beyond phosphorene.

Nowadays, the physical, chemical, electrical, and electrochemical properties of two-dimensional (2D) layered materials are intensely studied in the search for advanced applications in the nanoelectronics, energy, biomedical, and environmental fields.<sup>[1,2]</sup> Particularly for biomedical and environmental applications, researchers in the development of smart and sensitive optical and electrochemical biosensors have made tremendous gains recently<sup>[3–6]</sup> with respect to precious nanoparticles.<sup>[7]</sup> The most studied 2D materials for use as platforms or to label biosensor applications are graphene, metal transitional dichalcogenides (TMDs), and black phosphorus (BP), which demonstrate their promising capacity in the development of this field of research.<sup>[6,8–12]</sup> Following explosive interest in the study of phosphorene's physicochemical properties and applications,<sup>[9,13–16]</sup> current research focuses on other elements that adopt a layered structure such as arsenene, antimonene, and bismuthene. These Group VA elements are called "pnictogens" or "pnictides" (IUPAC recommended designation).<sup>[17–22]</sup> The heavier pnictogens have the advantage of a higher stability than phosphorene.<sup>[23]</sup> These pnictogens beyond BP are not much explored and scientific reports of their potential applications are currently limited, particularly in the field of biosensing. Recently, scalable and simple methods based on shear force exfoliation were developed by our group and the obtained exfoliated pnictogens show high electrochemical activity.<sup>[21–23]</sup> However, we believe that it is necessary to explore other applications of these materials such as biosensing. Herein, we optimized and implemented a phenol enzymatic biosensor where exfoliated pnictogens (phosphorene, arsenene, antimonene, and bismuthene) are used as a platform for enhanced electron transfer. Interestingly, antimonene shows the best performance and the resulting biosensor revealed high

analytical performance in term of sensitivity, selectivity, and reproducibility. Moreover, to the best of our understanding, it is the first example of a biosensing application reported for pnictogens beyond phosphorene.

A promising application for novel 2D pnictogens in an enzymatic biosensor was evaluate. Shear exfoliation method was used to obtain the pnictogens nanosheets (Scheme 1A). The biosensor device was constructed using a layer-by-layer method of each pnictogen (phosphorene, arsenene, antimonene, and bismuthene), enzyme (tyrosinase), and crosslinking agent (glutaraldehyde, Glu) (Scheme 1B). The obtained biosensor was used for phenol detection following the o-quinone electroreduction to catechol (Scheme 1C). Tyrosinase (Tyr) is the enzyme responsible for the two oxidation steps of phenol to catechol and catechol to o-quinone.



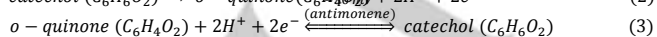
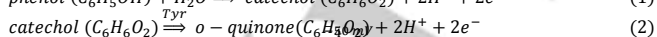
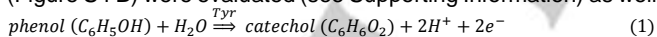
**Scheme 1.** (A) Shear exfoliated pnictogens using kitchen blender. (B) Biosensor preparation using layer-by-layer drop-casted pnictogen nanosheets, tyrosinase (Tyr), and glutaraldehyde (Glu) onto a glassy carbon (GC) electrode. (C) Chemical mechanism of phenol detection by biosensor based on exfoliated pnictogen and Tyr.

Once the layered pnictogens (P, As, Sb, Bi) were exfoliated, a structural and chemical characterization of their chemical composition and morphology was performed. Transmission electron microscopy (TEM) images (Figure 1: left and central panels) clearly show the extent of exfoliation and the lateral size of the exfoliated pnictogens. Interestingly, each material shows a different degree of exfoliation. Antimonene and phosphorene show the typical 2D structure of a few layers (Figure 1A and 1D). Antimonene displays well-defined nanosheets with lateral size of around 200 nm and underwent a substantial downsizing from the bulk. Large sheets of arsenene with a wrinkled structure were observed (Figure 1B) and agglomerated nanoparticles of bismuthene (Figure 1C) were obtained. Moreover, the selective area electron diffraction (SAED) patterns and HR-TEM images show the crystallinity corresponding to the rhombohedral (As, Sb, and Bi) and orthorhombic (BP) structures of the exfoliated pnictogens (see Figure 1: right panels and inset). The EDX

[a] Dr. C.C. Mayorga-Martinez, Dr. R. Gusmão, Prof. Dr. Z. Sofer, Prof. Dr. M. Pumera\*  
Center for Advanced Functional Nanorobots, Department of Inorganic Chemistry, University of Chemistry and Technology Prague, Technická 5, 166 28 Prague 6, Czech Republic  
E-mail: martin.pumera@vscht.cz  
Supporting information for this article is given via a link at the end of the document.

## COMMUNICATION

mapping from the TEM images (see Figure S1) confirmed the presence of the element for each pnictogen and the oxygen content. The bulk materials were also investigated by X-ray diffraction (spectra provided in Figure S2). All samples were single-phase corresponding to orthorhombic black phosphorus and rhombohedral arsenic, antimony, and bismuth. Within the arsenene was observed arsenic oxide due to partial oxidation, which means that the crystalline structure remains intact after the exfoliation process. The surface composition, chemical bonding of the bulk, and exfoliated pnictogens were evaluated by X-ray photoelectron spectroscopy (XPS) (see Figure S3 in SI). The exfoliated materials displayed a partial oxidation from the starting materials, but it is also interesting to mention that in the case of antimonene, its bulk shows a significant degree of oxidation in comparison with the other bulk materials (Bi, As, and BP). In this manner, the oxidation ratio of the antimonene is the lowest of the series.<sup>[23]</sup> After the exfoliated pnictogens were properly characterized, we proceeded to evaluate their applications as nanocarriers to enhance the activity of an enzyme-based phenol biosensor. In this manner, we fabricated and optimized the biosensing system using exfoliated pnictogens. First, we prepared different biosensors using each pnictogen and their electrocatalytic responses were measured by cyclic voltammetry (Figure 2A). The cyclic voltammograms (CVs) were carried out in phenol 200  $\mu\text{M}$  solution prepared in PBS pH 6.5. The catalytic activity of this phenol biosensor based on tyrosinase (Tyr) was electrochemically detected by the evaluation of a reduction peak corresponding to the electroreduction of *o*-quinone to catechol at negative low potentials (Scheme 1C). Particularly, in the phenol biosensor described here, the *o*-quinone reduction peak occurs at around  $-43$  mV for antimonene,  $-63$  mV for phosphorene,  $-30$  mV for bismuthene, and  $-4$  mV for arsenene; however, current intensity occurs in the following order: antimonene > phosphorene > bismuthene > arsenene. The electrochemical mechanism of this biosensor system is based on three successive reactions. First, phenol hydroxylation to catechol in presence of tyrosinase (reaction 1) followed by the catechol oxidation to *o*-quinone by tyrosinase (reaction 2) and, finally, the electro-reduction of *o*-quinone to catechol (reaction 3).<sup>[24]</sup> Remarkably, all the exfoliated materials show some reduction peak of *o*-quinone; however, antimonene (red curve) shows the best performance based in its current intensity. The role of each layer of the antimonene-based biosensor (Figure S4 A) and its response at different phenol concentrations (Figure S4 B) were evaluated (see Supporting Information) as well.



It is of importance to mention that the pnictogens show thiophilic characteristics, binding to the cysteine group of the proteins.<sup>[30]</sup> This is the reason that the enzyme molecules are well immobilized onto the pnictogens. It is well known that arsenic compounds are able to inhibit up to 200 enzymes.<sup>[26-28]</sup> Herein, when the arsenene was used as platform for this tyrosinase-based biosensor, the signal is lower (green line in Figure 2A) in comparison to the carbon biosensing platform (black dash line in Figure 2A). This is likely due to enzyme inhibition by arsenene. In contrary, antimonene shows enhanced signal (red line), which confirms that this material does not inhibit the enzyme activity.<sup>[29]</sup>

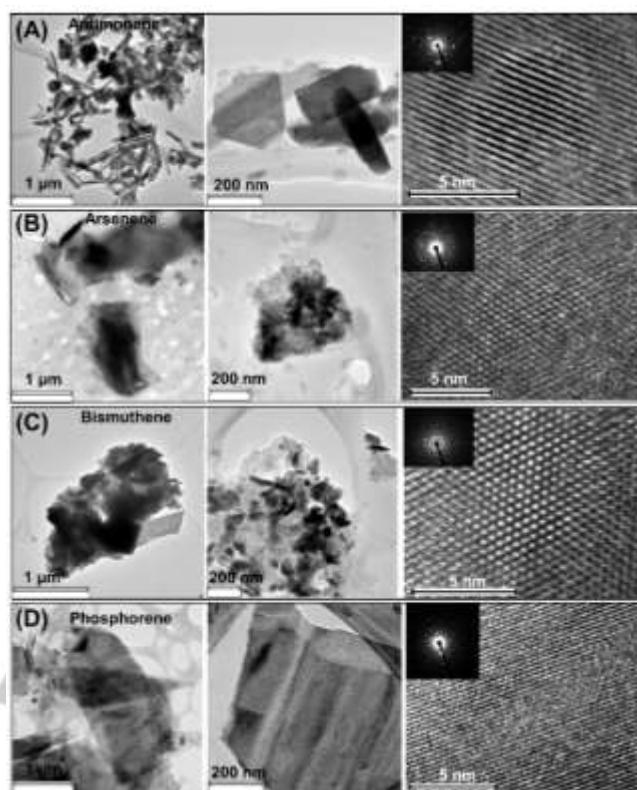


**Figure 1.** Transmission electron microscopy at different magnifications (left and central panels), high-resolution TEM (right panels), and selective area diffraction (insets) of antimonene (A), arsenene (B), bismuthene (C), and phosphorene (D) shear-exfoliated nanosheets.

Comparison with biosensors prepared using Sb bulk (red dash line) and glassy carbon electrode (black dash line) (Figure S5) shows the enhanced activity of the antimonene based biosensor for phenol detection. Moreover, similar signals for bulk layered Sb and GC were observed, which means that the enzyme activity is not inhibited by neither bulk nor exfoliated antimony. Bismuthene and phosphorene yielded signals similar to the control measurements (biosensor without pnictogens, Figure 3A), which demonstrates that although they do not inhibit their enzymatic activity, these materials have not improved the biosensor electroactivity. In order to elucidate the role of the antimonene in the observed enhanced signal in this biosensing system, different experiments were performed. First, the ability of the exfoliated pnictogens for *o*-quinone reduction to catechol was evaluated. GC electrodes were modified with each pnictogen and the electrochemical process of catechol oxidation to *o*-quinone<sup>[30,31]</sup> was evaluated, see Figure 2B. A single oxidation peak of catechol oxidation to *o*-quinone was observed around  $+0.35$  V and the peak corresponding to *o*-quinone reduction was observed at  $+0.11$  V during reversed scan. However, arsenene shows enhanced catechol oxidation (green line), whereas antimonene reduced the *o*-quinone to catechol more efficiently (red line). Secondly, the electroactivity of phenol in presence of pnictogens was also evaluated (Figure 2C). In this case, only an irreversible phenol oxidation peak at higher anodic potentials was observed for all pnictogens ca.  $+0.7$  V, thus demonstrating that the exfoliated pnictogens are not able to detect phenol without the presence of Tyr.

## COMMUNICATION

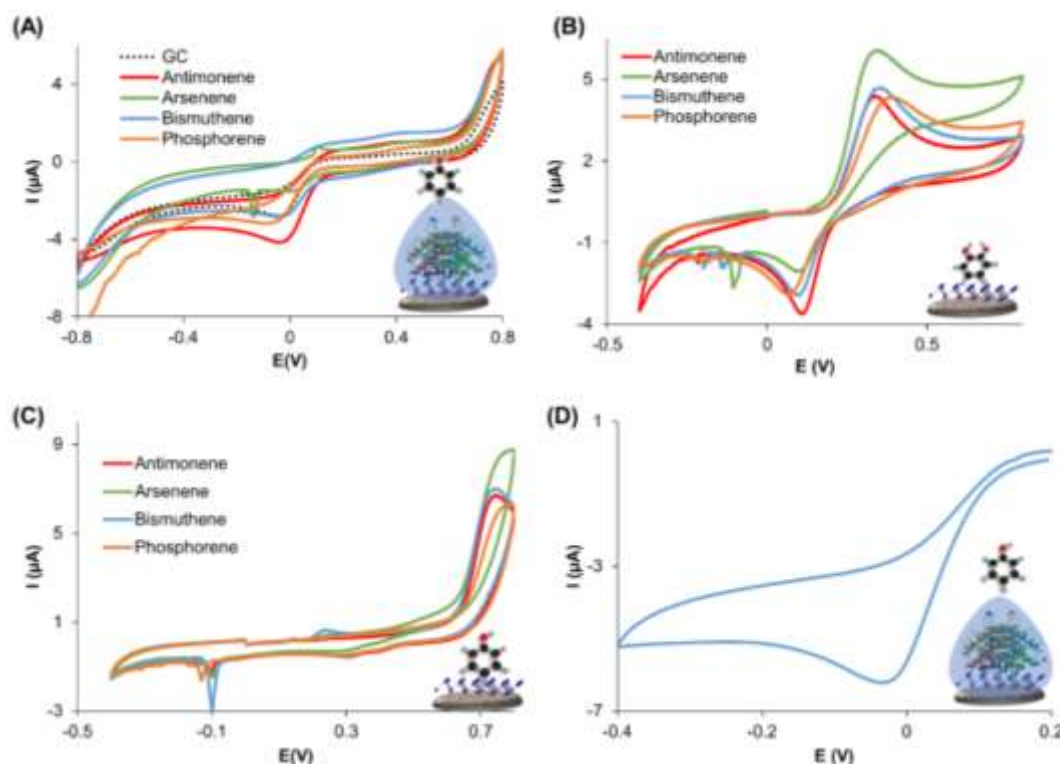


**Figure 2.** (A) CVs of biosensors based on phosphorene, arsenene, antimonene, and bismuthene for phenol (200  $\mu\text{M}$ ) detection. Electrochemical activity of the exfoliated pnictogens in presence of (B) catechol 200  $\mu\text{M}$  and (C) phenol 200  $\mu\text{M}$ . Experimental conditions: 0.1 M PBS pH 6.5, and scan rate 50 mV/s.

The enhanced performance of the antimonene-based phenol biosensor can be assigned to three factors: (i) a degree of exfoliation and downsizing as well-observed in the TEM images (Figure 1A), (ii) the lowest ratio of oxidation of its surface observed in the XPS studies (Figure S3) and (iii) the biocompatibility of antimonene (Figure 2A). These findings reveal antimonene with enhanced electron transfer capability suitable for biosensors application. Consequently, antimonene was the chosen exfoliated pnictogen for the fabrication of the phenol biosensor.

In a third sets of experiments, considering that the phenol detection in this biosensor system is based on *o*-quinone reduction, antimonene based biosensor was prepared and evaluated. Figure 2D shows cathodic voltammetric scan, from +0.2 to -0.4 V in presence of 200  $\mu\text{M}$  of phenol. The antimonene-based biosensor shows a cathodic peak at -0.01 V that corresponds to *o*-quinone reduction. This confirms that the *o*-quinone production and subsequent reduction by the antimonene-based biosensor is not dependent on any electro-oxidation pre-process. In contrast, anodic potentials oxidize phenol, thus competing with the enzyme for the substrate and decreasing the performance of the pnictogenene-based biosensor. CV was measured at different scan rates from 5 to 400 mV/s at the antimonene-based biosensor in presence of phenol 200  $\mu\text{M}$  to have an insight whether the process is diffusion or adsorption controlled (Figure S6). The reduction peak current (reaction 3) is proportional to the scan rate, which mean that this is an adsorption controlled electrochemical process.

We optimized the detection potential in wide range of potential (Figure S4 C in Supporting Information). Subsequently, once the most favorable working potential was optimized (-5 mV) the chronoamperogram of various phenol concentrations was recorded (Figure 3). Remarkably, we observed the current drop as a small step in the presence of 500 nM of phenol, demonstrating the high sensitivity of the biosensor implemented and electrochemical detection method used as well. This enzymatic biosensor system operates following the Michaelis-Menten kinetics scheme, see the current response vs. concentration plot (Figure S7 A). Calibration curves from chronoamperograms are shown in Figures S7 B and C. Calibration and analytical data are stated in the Supporting Information.

The phenol biosensor based on antimonene (antimonene/Tyr/Glu) showed good analytical performance with high sensitivity, selectivity, reproducibility, and specificity. Taking in account the high toxicity of phenolic compounds, which have an exposure limit of 5  $\mu\text{M}$  in drinking water,<sup>[32]</sup> this biosensor represents a good alternative for phenolic compound detection in environmental control applications as its LOD is 10 times lower than this limit. The influence of interferences (Figure S8 A) and the recoveries of spiked tap water (Figure S8 B and C) for its future application in real samples are discussed in Supporting Information. The sensitivity of this biosensor is comparable with

## COMMUNICATION

other reported tyrosinase biosensors based on 2D materials (see Supporting Information).

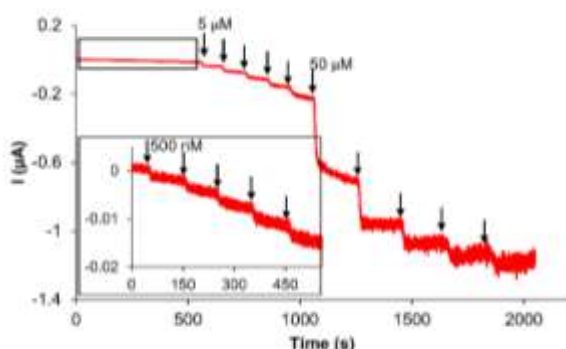


**Figure 3.** (A) Chronoamperometry response during the addition of different phenol concentrations at  $-5$  mV in  $0.1$  M PBS pH  $6.5$ .

In summary, we fabricated a biosensor based on thin nanosheets of 2D layered pnictogens (phosphorene, arsenene, antimonene, and bismuthene) obtained by shear force exfoliation as a platform for the detection of phenol. Exfoliated pnictogens undergo predominantly a downsizing process alongside with delamination to thin nanosheets. From the set of tested layered pnictogen, antimonene exhibited the highest degree of exfoliation and the lowest oxidation-to-bulk ratio. Simultaneously, the phenol biosensor based on antimonene shows enhanced analytical performance in terms of linearity, sensitivity, selectivity, and reproducibility compared with sensors based on other exfoliated group VA elements. The improved electrocatalytic reduction of phenol observed for the 2D layered antimonene/Tyr/Glu configuration offers a feasible mean toward its detection in the presence common interferents and in real samples. The antimonene/Tyr/Glu exhibited a phenol LOQ of  $850$  nM and an LOD of  $255$  nM, 10 times below its recommended limit.<sup>[33]</sup> The proposed exfoliated pnictogen-based biosensors showcases the great potential of these type of monoelemental layered materials in future biomedical and environmental sensing applications.

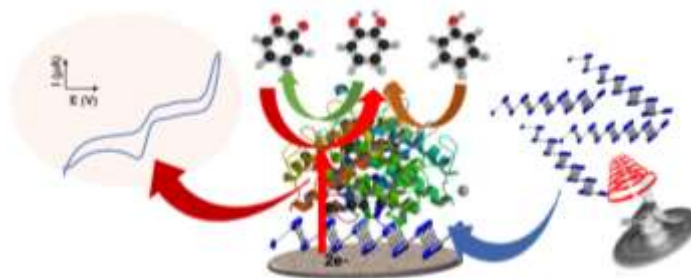
## Acknowledgements

Research was supported by the project Advanced Functional Nanorobots (reg. No. CZ.02.1.01/0.0/0.0/15\_003/0000444 financed by the EFRR). Z.S. is supported by the Czech Science Foundation (GACR No. 16-05167S). This work was created with the financial support of the Neuron Foundation for science support (Z.S.).

**Keywords:** Pnictogen, phosphorene, monoelemental layered material, electrochemical biosensor, toxic compound, phenol biosensor

- [1] C. Tan, X. Cao, X.-J. Wu, Q. He, J. Yang, X. Zhang, J. Chen, W. Zhao, S. Han, G.-H. Nam, M. Sindoro, H. Zhang, *Chem. Rev.* **2017**, *117*, 6225-6331.  
 [2] W. Choi, N. Choudhary, G. H. Han, J. Park, D. Akinwande, Y. H. Lee, *Mater. Today* **2017**, *20*, 116-130.

- [3] Y. Chen, C. Tan, H. Zhang, L. Wang, *Chem. Soc. Rev.* **2015**, *44*, 2681-2701.  
 [4] D. Chimene, D. L. Alge, A. K. Gaharwar, *Adv. Mater.* **2015**, *27*, 7261-7284.  
 [5] R. Kurapati, K. Kostarelos, M. Prato, A. Bianco, *Adv. Mater.* **2016**, *28*, 6052-6064.  
 [6] W. Wen, Y. Song, X. Yan, C. Zhu, D. Du, S. Wang, A. M. Asiri, Y. Lin, *Mater. Today*, **2017**, doi: j.mattod.2017.09.001.  
 [7] K. Saha, S. S. Agasti, C. Kim, X. Li, V. M. Rotello, *Chem. Rev.* **2012**, *112*, 2739-2779.  
 [8] C. C.; Mayorga-Martinez, B. Khezri, A. Y. S. Eng, Z. Sofer, P. Ulbrich, M. Pumera, *Adv. Funct. Mater.* **2016**, *26*, 4094-4098.  
 [9] M. Pumera *Trends Anal. Chem.* **2017**, *93*, 1-6.  
 [10] R. J. Toh, C. C. Mayorga-Martinez, Z. Sofer, M. Pumera, *Adv. Funct. Mater.* **2017**, *27*, 1604923 1-8.  
 [11] M. Z. M. Nasir, C. C. Mayorga-Martinez, Z. Sofer, M. Pumera, *ACS Nano*, **2017**, *11*, 5774-5784.  
 [12] C. C. Mayorga-Martinez, N. M. Latiff, A. Y. S. Eng, Z. Sofer, M. Pumera, *Anal. Chem.* **2016**, *88*, 10074-10079.  
 [13] R. Gusmão, Z. Sofer, M. Pumera *Angew. Chem. Int. Ed.* **2017**, *56*, 8052-8072.  
 [14] S.-Y. Cho, Y. Lee, H.-J. Koh, H. Jung, J.-S. Kim, H.-W. Yoo, J. Kim, H.-T. Jung, *Adv. Mater.* **2016**, *28*, 7020-7028.  
 [15] W. Lei, G. Liu, J. Zhang, M. Liu, *Chem. Soc. Rev.*, **2017**, *46*, 3492-3509.  
 [16] M. Z. Rahman, C. W. Kwong, K. Davey, S. Z. Qiao, *Energy Environ. Sci.*, **2016**, *9*, 709-728.  
 [17] M. Fortin-Deschênes, O. Waller, T. O. Mendes, A. Locatelli, S. Mukherjee, F. Genuzio, P. L. Levesque, A. Hebert, R. Martel, O. Moutanabbir, *Nano Lett.* **2017**, *17*, 4970-4975.  
 [18] M. Pumera, Z. Sofer, *Adv. Mater.* **2017**, *29*, 1605299 (2-8).  
 [19] L. Lu, Z. Liang, L. Wu, Y. Chen, Y. Song, S. C. Dhanabalan, J. S. Ponraj, B. Dong, Y. Xiang, F. Xing, D. Fan, H. Zhang, *Laser Photonics Rev.* **2018**, *12*, 1700221 (1-10).  
 [20] L. Lu, W. Wang, L. Wu, X. Jiang, Y. Xiang, J. Li, D. Fan, H. Zhang, *ACS Photonics*, **2017**, *4*, 2852-2861.  
 [21] R. Gusmão, Z. Sofer, D. Bouša, M. Pumera *Angew. Chem. Int. Ed.* **2017**, *56*, 14417-14422.  
 [22] W. Tao, X. Ji, X. Xu, M. A. Islam, Z. Li, S. Chen, P. E. Saw, H. Zhang, Z. Bharwani, Z. Guo, J. Shi, O. C. Farokhzad, *Angew. Chem. Int. Ed.* **2017**, *56*, 11896-11900.  
 [23] R. Gusmão, Z. Sofer, D. Bouša, M. Pumera, *ACS Appl. Energy Mater.* **2018**, *1*, 503-509.  
 [24] Z. Liu, B. Liu, J. Kong, J. Deng, *Anal. Chem.* **2000**, *72*, 4707-4712.  
 [25] C. Nitsche, M. C. Mahawaththa, W. Becker, T. Huber, G. Otting, *Chem. Commun.*, **2017**, *53*, 10894-10897.  
 [26] J. L. Webb, In *Enzyme and Metabolic Inhibitors* Academic Press: New York, 1966; Vol. III, p 595.  
 [27] S. Shen, X. F. Li, W. R. Cullen, M. Weinfeld, X. C. Le, *Chem. Rev.*, **2013**, *113*, 7769- 7792.  
 [28] V. S. Chang, S. S. Teo, *Int. Food Res. J.* **2016**, *23*, 2370-2373.  
 [29] R. E. Gyurcsányi, Z. Vágföldi, K. Tóth, G. Nagy, *Electroanalysis* **1999**, *11*, 712-718.  
 [30] Q. Lin, Q. Li, C. Batchelor-McAuley, R. G. Compton, *J. Phys. Chem. C*, **2015**, *119*, 1489-1495.  
 [31] L. Chen, X. Li, E. E. L. Tanner, R. G. Compton, *Chem. Sci.*, **2017**, *8*, 4771-4778.  
 [32] S. J. Kulkarni, R. W. Tapre, S. V. Patil, M. B. Sawarkar, *Procedia Eng.* **2013**, *51*, 300-307.  
 [33] <http://apps.who.int/iris/bitstream/10665/39958/1/9241510889-eng.pdf>, IPCS International Programme on Chemical Safety, Health and Safety Guide No. 88, Phenol Health and Safety Guide, World Health Organization, Geneva 1994 (accessed 5 March 2018).

**COMMUNICATION**  
**COMMUNICATION****Keyword: Biosensing***Carmen C. Mayorga-Martinez, Rui Gusmão, Zdeněk Sofer, and Martin Pumera**Page No. – Page No.***Pnictogens Based Biosensor: Phosphorene, Arsenene, Antimonene, and Bismuthene**

Highly sensitive and selective phenol biosensor using 2D antimonene as a platform.

WILEY-VCH

Accepted Manuscript